

## Degradation Behaviour of Aluminium in 2M HCl/HNO<sub>3</sub> in the Presence of *Arachis hypogaea* Natural Oil

A. P. I. Popoola\*, O. S. I. Fayomi, M. Abdulwahab

Department of Chemical and Metallurgical Engineering, Tshwane University of Technology, Pretoria, P.M.B. X680, South Africa 0001

\*E-mail: [popoolaapi@tut.ac.za](mailto:popoolaapi@tut.ac.za)

Received: 16 May 2012 / Accepted: 11 June 2012 / Published: 1 July 2012

---

Studies have been made on the corrosion inhibition of aluminium alloy in 2M HCl and HNO<sub>3</sub>/*Arachis hypogaea* natural oil using gravimetric and potentiodynamic polarization techniques at 25°C. The results revealed that *Arachis hypogaea* oil in 2M HCl and HNO<sub>3</sub>-aluminium environment decreased the corrosion rate at various concentrations considered. Higher inhibitor efficiency (IE) of 83.48, 96.24 and 95.57% using potentiodynamic polarization methods were demonstrated in HCl solution at 20, 50 and 100%v/v *Arachis hypogaea*. While an IE of 99.03, 99.94 and 88.55% were recorded at 20, 50 and 100%v/v *Arachis hypogaea* respectively. The IE using the gravimetric method for both aluminium-HCl/HNO<sub>3</sub>-*Arachis* 20, 50 and 100%v/v *Arachis hypogaea* was significantly enhanced. The scanning electron microscope (SEM) surface morphology of as-corroded uninhibited condition showed severe damage and pits formation than as-corroded inhibited conditions. The additions of *Arachis hypogaea* as corrosion inhibitor indicate a high potential value, IE and polarization resistance with decreased in current density. The methods for the corrosion assessment of the aluminium were in agreement and a mixed-type corrosion exist which obeyed Langmuir adsorption isotherms.

---

**Keywords:** Aluminium, *Arachis hypogaea*, interface, surface morphology, SEM-EDS

### 1. INTRODUCTION

Aluminium and its alloy are widely used for different applications in the industries and marine environment because of their excellent properties [1-3]. Generally, aluminium has higher corrosion resistance because of its thin surface oxide film formation. Although, in an aggressive environment, mostly chloride and acidic, the protective films breaks, however, the oxide coating is not totally removed but is thinned and regenerate by the oxidation of the underlying metal [4]. Moreover, in these aggressive medium, the regeneration of the thin film layer may be delayed and an active region is created, hence pits are initiated and may propagate further. The use of inhibitors has been reported to

offer protection for metals and alloys in most environments. Over the years, this has been subject of interest in corrosion science and engineering research area [5-7]. Some chemical and synthetic corrosion inhibitors that have been known to exhibit good corrosion resistance are not eco-friendly and create environmental threat [8-11]. Therefore, efforts toward identifying any potential eco-friendly and less expensive corrosion inhibitors remain relevant and progressive. Although the growing interest among researchers for a green inhibitors remained a top research focus. In that direction, plant extracts and oils has gained acceptance as corrosion inhibitors that are considered safe, eco-friendly, available and less expensive for most metals and alloys [9]. In view of this, we considered it necessary in this work, to study the potential of natural Peanut oil (*Arachis hypogaeae*) as corrosion inhibitor for aluminium alloy in 2M HCl and HNO<sub>3</sub> acidic media using gravimetric and potentiodynamic polarization methods.

## 2. EXPERIMENTAL PROCEDURES

### 2.1 Materials and sample preparation

Aluminium alloy specimen of dimension 20 x 20 x 3 mm with chemical composition shown in Table 1 was used as coupons for the corrosion study in 2M hydrochloric acid (HCl) and nitric acid (HNO<sub>3</sub>) solution. Initially, the coupons were mechanically polished with emery papers down to 600. The samples were degreased in ethanol, dried, weighed and stored in a desiccator. The initial weight of each sample was taken and recorded. In each of hydrochloric and nitric acid, 2M concentration was prepared fresh as required for each experiment. The natural peanut oil (*Arachis hypogaeae*) used was obtained from Technology Innovation Agency, Chemical Station, Ga-Rankuwa, TUT, Pretoria with molecular structure shown in Figure 1. Corrosion studies were conducted at room temperature (25°C).

**Table 1.** Chemical composition of the aluminium alloy used

Element	Al	Si	Mn	Mg	Sr	Bi	Ca	Na	Fe	Ti	P, Cr, Zr,Cu,Zn	B,Ni,Ag, Co
%	99.01	0.157	0.025	0.5	0.0001	0.0024	0.0012	0.001	0.281	0.0046	0.01	0.004

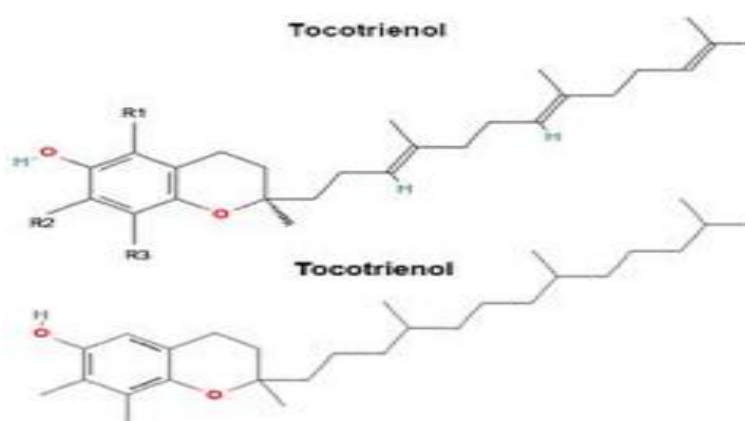


**Figure 1.** Molecular structure of Peanut oil (*Arachis hypogaeae*)

## 2.2 Gravimetric measurement

The gravimetric corrosion test was carried out on the previously weighed samples with and without inhibitor at 25°C. The volume of the solution was 100 ml with and without the addition of *Arachis hypogaeae* inhibitor. The *Arachis hypogaeae* inhibitor concentration (C) was varied from 20, 50 and 100% v/v in 100 ml of 2M HCl and HNO<sub>3</sub> acidic solution. For each sample, using gravimetric method, the samples were washed, dried and weight taken at interval of 12, 24 and 36 h of exposure time. The corrosion rate and inhibitor efficiency were determined along with the degree of surface coverage for each inhibitor concentration at 25°C.

## 2.3 Electrochemical measurement

The potentiodynamic polarization was used to characterize the corrosion rate of the aluminium in *Arachis hypogaeae*-acidic media. In the electrochemical test, a glass corrosion cell kit with a platinum counter electrode, a saturated Ag/Ag reference electrode and aluminium sample as working electrode were used. The working electrodes samples were positioned at the glass corrosion cell kit, leaving 1 cm<sup>2</sup> surfaces in contact with the solution. Polarization test were carried out in two different solutions consisting of 2M HCl and HNO<sub>3</sub> at room temperature using a potentiostat. The polarization curves were determined by stepping the potential at a scan rate of 0.003V/sec. The polarization curves were plotted using Autolab data acquisition system (Autolab model: AuT71791 and PGSTAT 30), and both the corrosion rate and potential were estimated by the Tafel extrapolation method using both the anodic and cathodic branches of the polarization curves.

## 2.4 Surface morphology

The surface morphology of as-corroded uninhibited and inhibited aluminium sample were examined with scanning electron microscopy equipped with energy dispersive spectroscopy to analyze the elements in the surface (model: Joel 6100).

# 3. RESULTS AND DISCUSSION

## 3.1 Results

The gravimetric corrosion data for aluminium in 2M HCl and HNO<sub>3</sub> along with the variation in inhibitor concentration can be found in Table 2, Figures 2 and 3. Tables 3 and 4 show the electrochemical corrosion parameters obtained for aluminium-2M HCl and HNO<sub>3</sub>/*Arachis hypogaeae* interface. Figures 4 and 5 depict the polarization curves for aluminium-2M HCl and HNO<sub>3</sub>/*Arachis hypogaeae* respectively. The surface morphology of as-corroded uninhibited/inhibited aluminium in 2M HCl and HNO<sub>3</sub>/*Arachis hypogaeae* are presented in Figures 6-9. In Figures 10 and 11, the percentage

inhibitor efficiency (%IE) for *Arachis hypogaea* using different methods for corrosion assessment were computed. Figure 12 demonstrated the adsorption isotherms for the two environments under this study.

### 3.2 Discussion

#### 3.2.1 Gravimetric measurement

An acidic environment consisting of 2M HCl and HNO<sub>3</sub> solutions were considered separately for corrosion behaviour of aluminium-*Arachis hypogaea* at different inhibitor concentrations at 25°C. Results show that corrosion rate (CR) of aluminium decreased with addition of *Arachis hypogaea* as an eco-friendly corrosion inhibitor for both environments and exposure time of 12, 24 and 36 h (Table 2, Figures 2 and 3). For 2M HCl-*Arachis hypogaea* interface, at various exposure times, corrosion rate decreased, though with lower percentage inhibitor efficiency (% IE). Specifically, Figure 2 shows a decrease in corrosion rate with concentration of inhibitor for all the immersion time at 25°C. Equally in 2M HNO<sub>3</sub>-*Arachis hypogaea* interface, similar trends were demonstrated with much higher corrosion resistance throughout the exposure time (Figure 3). In this case, a higher % IE was evidenced by the natural oil as the exposure time increases. Considering an exposure time of 12 h, higher % IE was calculated to be 92.37% at 50%v/v *Arachis hypogaea* addition. While at 20%v/v inhibitor concentration for 24 and 36 h exposure time, corrosion rate/IE were found to be 0.00151/81.61% and 0.00163/78.28% respectively.

**Table 2.** Corrosion rate (CR), Inhibition efficiency and surface coverage ( $\theta$ ) for aluminium in 2M HCl and 2M HNO<sub>3</sub> solution without and with varying concentration of *Arachis hypogaea* (%v/v) at 25°C

Time(hr)	C (% v/v)	CR 2M HCl (mm/day)	CR 2M HNO <sub>3</sub> (mm/day)	Surface coverage ( $\theta$ ) for HNO <sub>3</sub>	Inhibition Efficiency (%) for HNO <sub>3</sub>
12	0	0.05330	0.01720	-	-
	20	0.03300	0.00193	0.8875	88.75
	50	0.04960	0.00131	0.9237	92.37
	100	0.02880	0.00183	0.8900	89.00
24	0	0.07980	0.96800	-	-
	20	0.07740	0.00151	0.8161	81.61
	50	0.07410	0.00494	0.4002	40.02
36	0	0.06400	0.00591	0.2828	28.29
	0	0.05390	0.99900	-	-
	20	0.06180	0.00163	0.7828	78.28
	50	0.05650	0.00954	-0.2671	-26.71
	100	0.05380	0.00872	-0.1585	-15.85

However, corrosion resistance of aluminium in HNO<sub>3</sub>-*Arachis hypogaea* is much higher than that in HCl- *Arachis hypogaea*. The occurrences have been attributed to the formation of thin oxides as

evidenced in the EDS (Figures 7-9) which interfered with the anodic and cathodic reactions. Therefore formation of pits and their growth becomes difficult. The thin layer of the oxides adhered to the metal surface resulting into a decrease in the corrosion rate. Similar results have been reported [3,12-15].

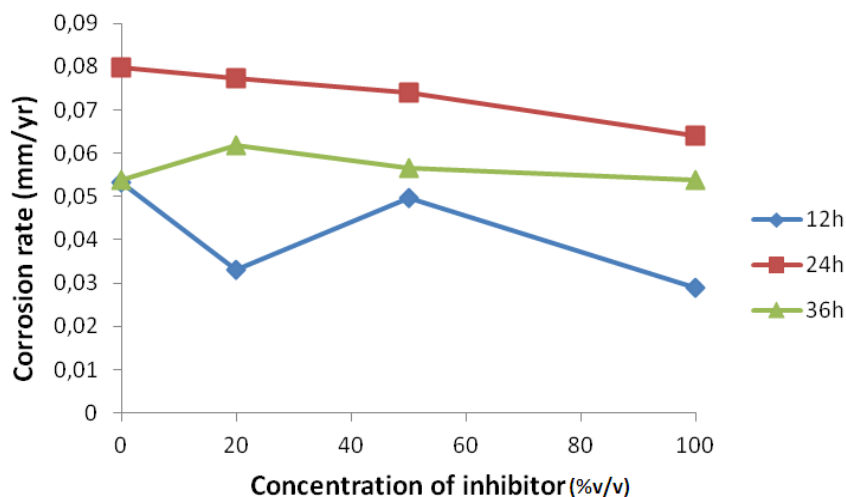


**Figure 2.** Variation of corrosion rate with concentration of inhibitor (% v/v) for aluminium in 2M HCl for different exposure time at 25°C

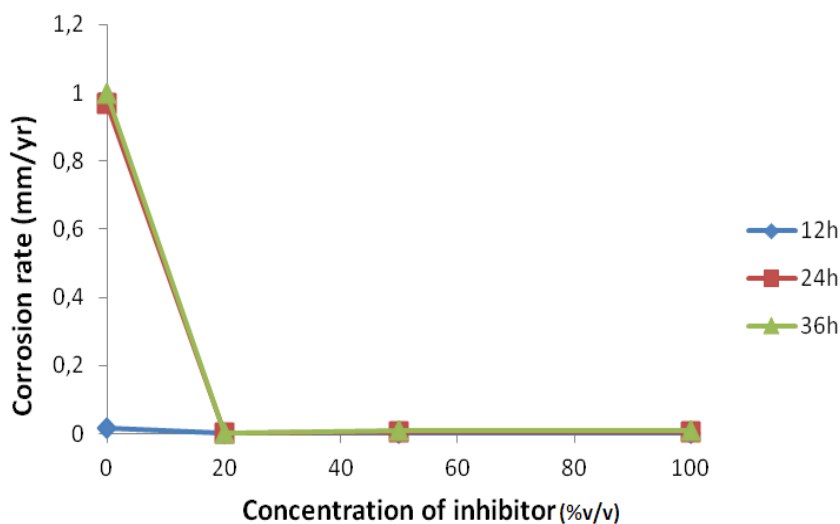


**Figure 3.** Variation of corrosion rate with concentration of inhibitor (%v/v) for aluminium in 2M HNO<sub>3</sub> for different exposure time at 25°C

### 3.2.2 Potentiodynamic polarization

From the potentiodynamic measurement for HCl and HNO<sub>3</sub>/ *Arachis hypogaeae* (Tables 3 and 4), potentiodynamic polarization-corrosion rate (PP-CR), potentiodynamic polarization-corrosion current (PP-I<sub>corr</sub>), and linear polarization resistance (LPR) were used as criteria for evaluating the

corrosion resistance of aluminium in the environments. Figures 4 and 5 indicate the polarization curves for 2M HCl and HNO<sub>3</sub>- *Arachis hypogaeae* at 25°C.

**Table 3.** Electrochemical corrosion data obtained for aluminium in 2M HCl-*Arachis hypogaeae* environment at 25°C

S/N	C (% v/v)	I <sub>corr</sub> (A/cm <sup>2</sup> )	ba (v/dec)	LPR R <sub>p</sub> (Ωcm <sup>2</sup> )	-E <sub>corr</sub> (V)	CR (mm/yr)
1	0	9.399E-5	0.015	3.658E-1	0.803	9.374E-1
2	20	1.553E-5	0.013	1.538E+0	0.774	1.549E-1
3	50	3.535E-6	0.005	1.907E+0	0.677	3.525E-2
4	100	4.159E-6	0.012	3.452E+0	0.772	4.148E-2

**Table 4.** Electrochemical corrosion data obtained for aluminium 2M HNO<sub>3</sub>-*Arachis hypogaeae* environment at 25°C

S/N	C (% v/v)	I <sub>corr</sub> (A/cm <sup>2</sup> )	ba (v/dec)	LPR R <sub>p</sub> (Ωcm <sup>2</sup> )	-E <sub>corr</sub> (V)	CR (mm/yr)
1	0	8.173E-7	0.022	4.215E+1	0.555	8.151E-3
2	20	7.935E-9	0.004	4.240E+2	0.254	7.913E-5
3	50	5.164E-10	0.018	6.072E+4	0.226	5.150E-6
4	100	9.358E-8	0.006	1.160E+2	0.397	9.333E-4

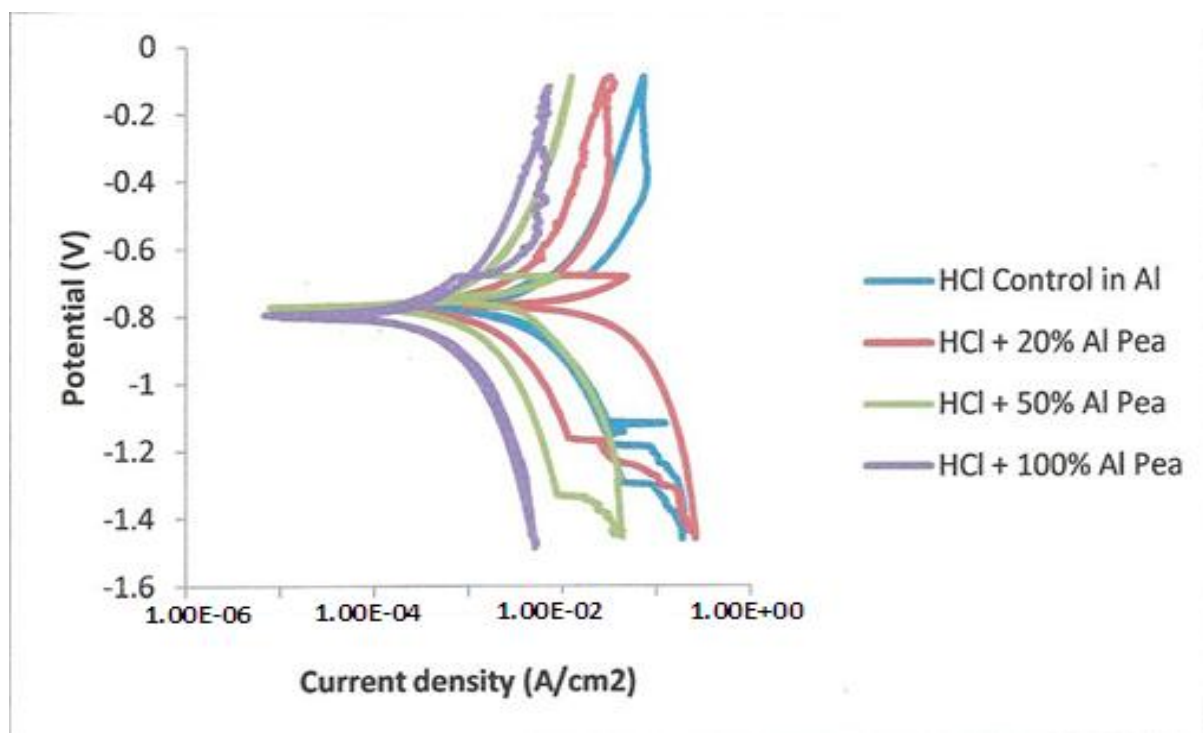


**Figure 4.** Linear polarization of aluminium in 2M HCl solution/*Arachis hypogaeae* environment at 25°C

Generally, both environments demonstrated a decreased corrosion rate and current density with addition of *Arachis hypogaea* inhibitor at all concentrations. While the corrosion potential ( $E_{\text{corr}}$ ) and polarization resistance ( $R_p$ ) increases with inhibitors concentrations. This is in agreement with previous studies [16,17]. The inhibited aluminium in HCl showed that corrosion rate decreased from 0.9374 mm/yr to 0.1549, 0.03525 and 0.04148 mm/yr at 20, 50, and 100%v/v *Arachis hypogaea* additions. While in  $\text{HNO}_3$  environment, corrosion rate decreased from 0.008151 mm/yr to 0.00007913, 0.00000515, and 0.0009333 mm/yr at 20, 50, and 100%v/v *Arachis hypogaea* respectively. It is important to note that corrosion resistance of aluminium-  $\text{HNO}_3$ -*Arachis hypogaea* interface is much higher than that of HCl-*Arachis hypogaea* interface with IE of 99.96% obtained at 50%v/v *Arachis hypogaea* addition for PP and 92.37% at 12 h for GM. However, based on the changes in anodic and cathodic branches for both environments, the mixed-type corrosion inhibition has been proposed.

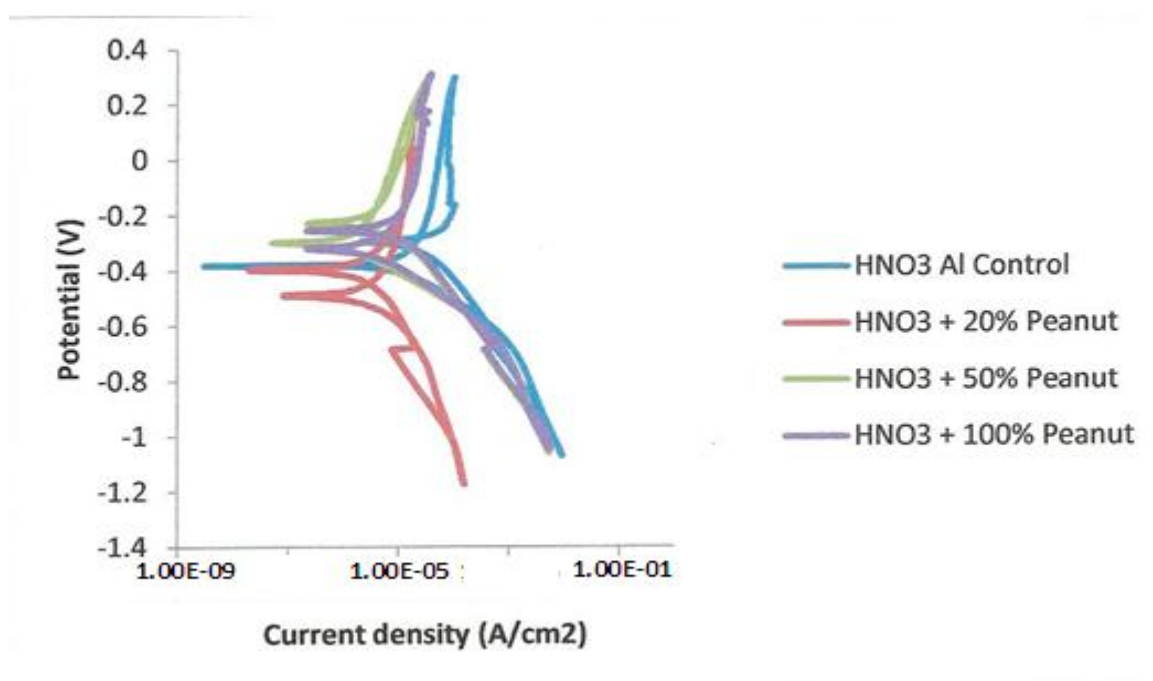


**Figure 5.** Linear polarization of aluminium in 2M  $\text{HNO}_3$  solution/*Arachis hypogaea* environment at 25°C

### 3.2.3 Scanning electron microscope-Energy dispersive spectroscopy (SEM-EDS)

From the surface morphology of uninhibited aluminium-HCl interface in Figure 6, severe pits, cracks and selective dissolution of intermetallic occurred at the surface after 12 h exposure time as compared with Figures 7, 8 and 9. In Figures 7 and 8, effect of exposure time of 12 and 36 h were assessed on the aluminium surface, results showed that higher exposure time of 36 h for HCl-50%v/v *Arachis hypogaea* (Figure 8) indicates surface degradation and pit formation than lower exposure time of 12 h under the same condition (Figure 7). This however, differs from  $\text{HNO}_3$ -50%v/v *Arachis*

*hypogaeae* (Figure 9), which correspond to the lower corrosion rate obtained from the linear polarization analysis.

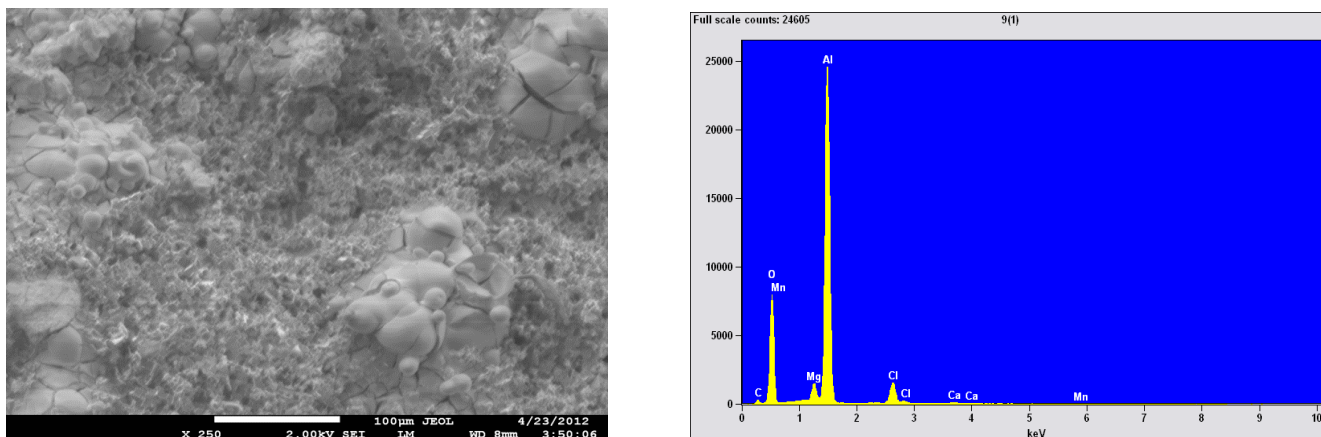


**Figure 6.** SEM micrograph of uninhibited aluminium in 2M HCl solution after 12 h with EDS

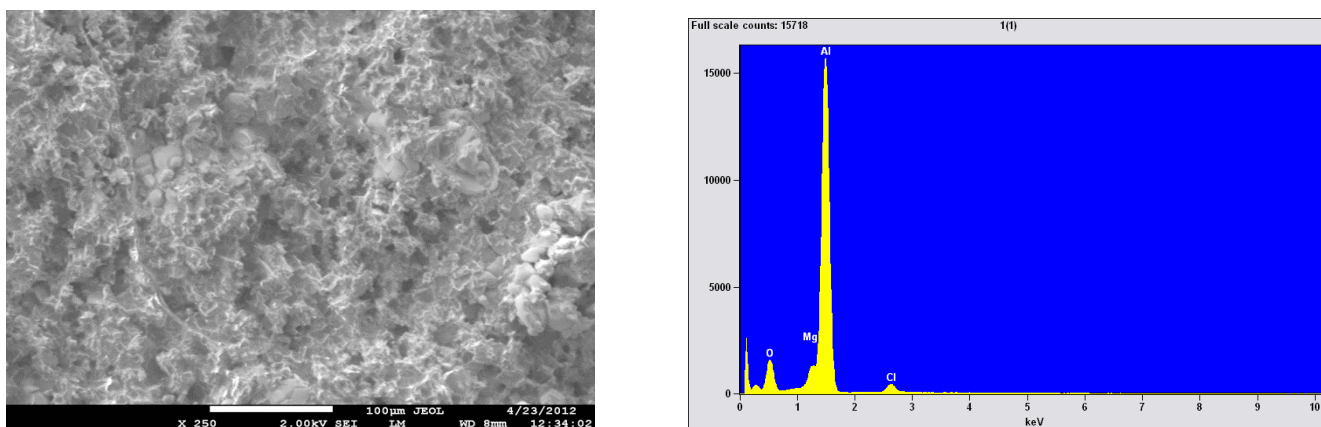


**Figure 7.** SEM micrograph of aluminium in 50%v/v *Arachis hypogaeae* -2M HCl solution after 12 h immersion time with the EDS

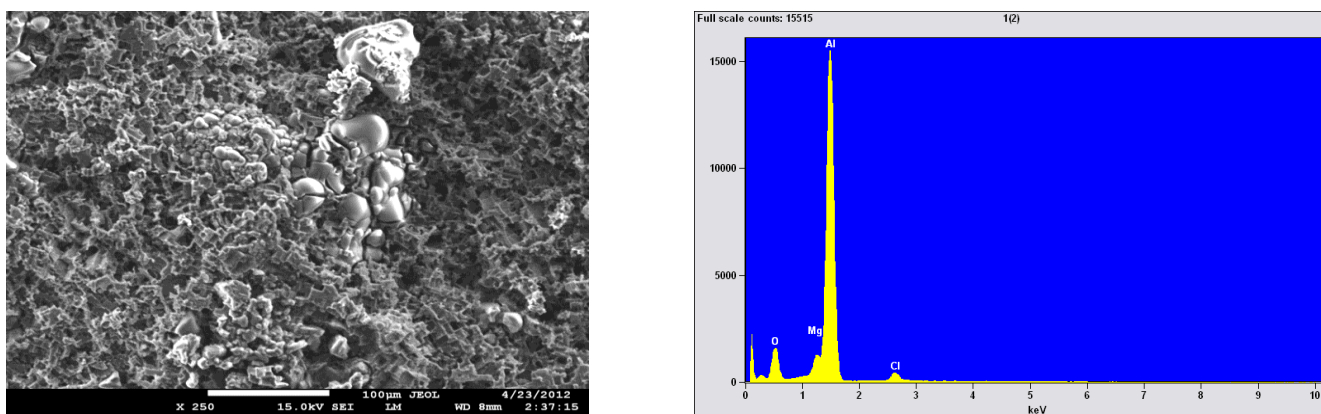


**Figure 8.** SEM micrograph of aluminium in 50%v/v *Arachis hypogaeae* -2M HCl solution after 36 h exposure time with the EDS



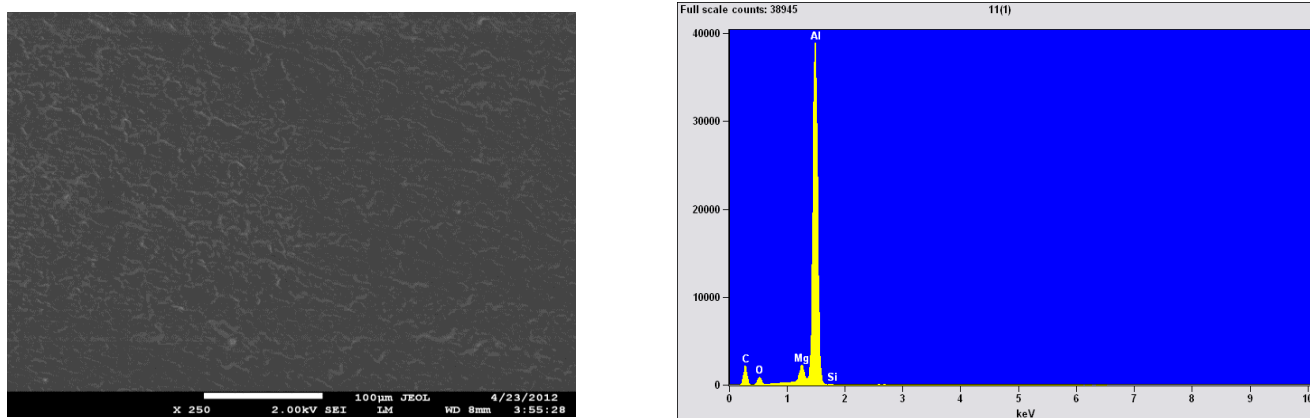


**Figure 9.** SEM micrograph of aluminium in 50% v/v *Arachis hypogae*-2M HNO<sub>3</sub> solution after 36 h immersion time with EDS

### 3.2.4 Inhibitor efficiency and adsorption behaviour

The percentage inhibitor efficiency (% IE) of the aluminium-*Arachis hypogae* in both HCl and HNO<sub>3</sub> solution were computed using the equation reported [9]. The variation in the %IE using gravimetric (GM), potentiodynamic polarization-corrosion rate (PP-CR), potentiodynamic polarization-corrosion density (PP-I<sub>corr</sub>), and linear polarization resistance (LPR) are presented in Figures 10 and 11 for 2M HCl and HNO<sub>3</sub>/*Arachis hypogae* respectively. The results show that % IE of the *Arachis hypogae* natural oil increases with an increase in the inhibitor concentrations. The reason being that, as the inhibitor concentration increases, the surface area covered by this inhibitor increased hence higher IE was achieved. *Arachis hypogae* oil can be said to exhibit a mixed-type corrosion inhibition because of the simultaneous change in the anodic and cathodic region during electrochemical measurement.

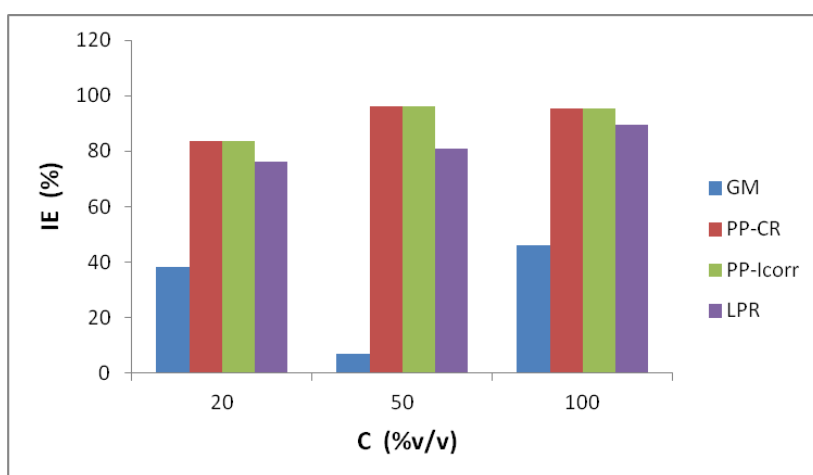


**Figure 10.** Comparative chart of inhibitor efficiency (IE) for aluminium-2M HCl solution/*Arachis hypogae* concentration obtained by gravimetric at 12 h (GM), potentiodynamic polarization-corrosion rate (PP-CR), potentiodynamic polarization-corrosion current (PP-I<sub>corr</sub>) and linear polarization resistance (LPR)

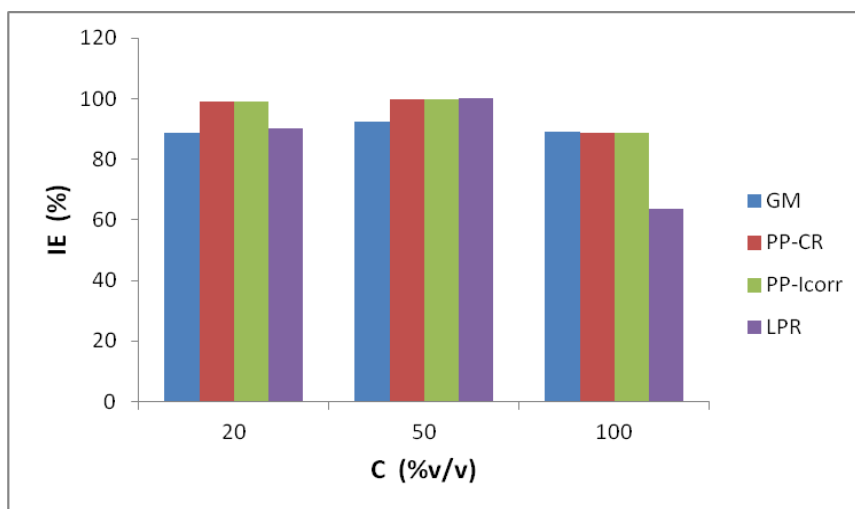


**Figure 11.** Comparative chart of inhibitor efficiency (IE) for aluminium-2M HNO<sub>3</sub> solution/*Arachis hypogae* concentration obtained by gravimetric at 12 h (GM), potentiodynamic polarization-corrosion rate (PP-CR), potentiodynamic polarization-corrosion current (PP-Icorr) and linear polarization resistance (LPR)

This is in agreement with previous studies [1,9]. However, there seems to be little agreement with GM and potentiodynamic polarization techniques for 2M HCl-*Arachis hypogae*/aluminium as against those observed in 2M HNO<sub>3</sub>-*Arachis hypogae*/aluminium condition. The adsorption mechanism has been demonstrated with a relationship between  $C/\theta$  and  $C$  that shows linearity at 25°C for both the environments (Figure 12). Since the correction factors ( $R^2$ ) are almost unity: HCl- PP-Icorr/PP-CR (0.999), LPR (0.9978) and HNO<sub>3</sub>- GM (0.9993), PP-Icorr/PP-CR (0.9988) .The adsorption behaviour is believed to have obeyed Langmuir adsorption isotherms.

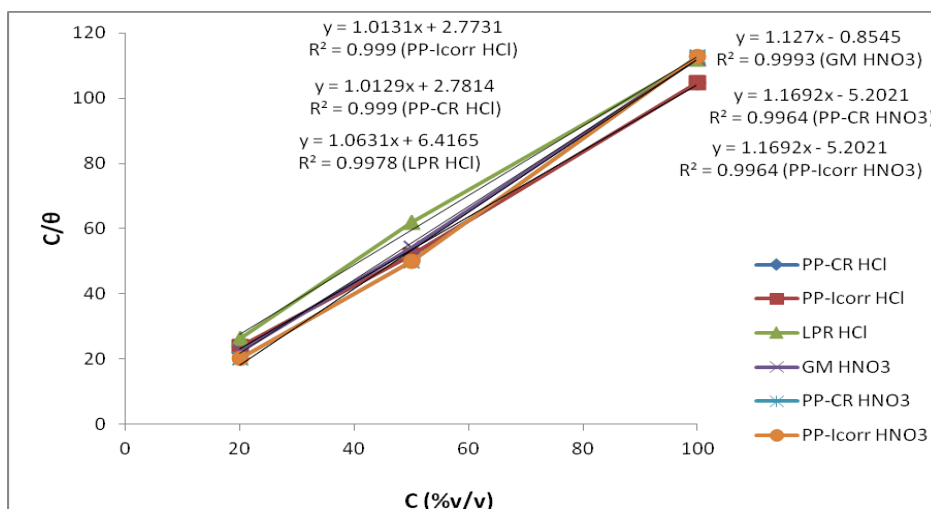


**Figure 12.** Langmuir isotherm for the adsorption of *Arachis hypogae* compounds on the aluminium surface in 2M HCl and HNO<sub>3</sub> solution at 25°C obtained by gravimetric and potentiodynamic polarization methods

#### 4. CONCLUSIONS

1. *Arachis hypogaea* have been demonstrated to be a good corrosion inhibitor for aluminium in 2M (HCl and HNO<sub>3</sub>) environments at 25°C
2. The corrosion rate of aluminium decreased with addition of *Arachis hypogaea* as inhibitor and enhanced inhibitor efficiency as high as 99.96% in HNO<sub>3</sub>-*Arachis hypogaea* condition was achieved.
3. Surface morphology of uninhibited aluminium sample shows severe pits and cracks
4. That the mixed-type corrosion inhibition exists and Langmuir adsorption isotherms were demonstrated for the aluminium alloy.

#### ACKNOWLEDGEMENTS

This material is based upon work supported financially by the National Research Foundation. The Technology Innovation Agency, Chemical Station, Ga-Rankuwa, TUT, is appreciated for equipment support.

#### References

1. R. Rosliza, W. B. W. Nik, *Current Applied Physics* 10 (2010) 221.
2. M. Abdulwahab, I.A. Madugu, S. A. Yaro, A. P. I. Popoola, *Silicon*, 4 (2) (2012) 137.
3. O. O. Ajayi, O. A. Omotosho, K. O. Ajanaku and B. O. Olawore, *Env. Res. J.* 5(4) (2011) 163.
4. M.A. Amin, H. H. Hassan, O. A. Hazzazi, M. M. Qhatani, *J Appl Electrochem.* 38 (2008) 1589.
5. D. B. Hmamou, R. Salghi, A. Zarrouk, B. Hammouti, S. S. Al-Deyab, Lh. Bazzi, H. Zarrok, A. Chakir, L. Bammou, *Int. J. Electrochem. Sci.* 7 (2012) 2361.
6. M. Sangeetha, S. Rajendran, T. S. Muthumegala, A. Krishnaveni, *Zastita Materijala* 52 (2011) 3.
7. V. S. Saji, *Recent Patents on Corrosion Science* 2 (2010) 6.
8. A. A. El-Meligi, *Recent Patents on Corrosion Science*, 2 (2010) 22.
9. J. Halambek, K. Berkovic, J. Vorkapic-Furac, *Corrosion Science* 52 (2010) 3978.
10. S. A. Umoren, I. B. Obot, E. E. Ebenso, P. C. Okafor, O. Ogbode, E. E. Oguzie, *Anti-Corrosion Methods and Materials* 53 (2006) 277.
11. S. A. Umoren, I. B. Obot, E. E. Ebenso, P. C. Okafor, *Portugaliae Electrochemica Acta* 26 (2008) 267.
12. I. B. Obot, S. A. Umoren, N. O. Obi-Egbedi, *J. Mater. Env. Sci.* 2(1) (2011) 60.
13. O. K. Abiola, J. O. E. Otaigbe, O. J. Kio, *Corrosion Science* 51 (2009) 1879.
14. S. A. Umoren, E. E. Ebenso, *Pigment and Resin Technology* 37 (2008) 173.
15. A. M. Al-Turkustani, M. M. Al-Solmi, *Journal of Asian Scientific Research* 1(7) (2011) 346.
16. A. M. Muhammed, H. H. Hamdy, H. A. Omar, M. Q. Mohsen, *J. Appl. Electrochem.* 38 (2011) 1589.
17. R. Rosliza, A. Nora'aini, W. B. W. Nik, *J. Appl. Electrochem.* 40 (2010) 833.